

Critical holes in undercooled wetting layers

G. Foltin¹, R. Bausch, R. Blossey

Institut für Theoretische Physik IV, Heinrich–Heine–Universität Düsseldorf,
Universitätsstraße 1, D-40225 Düsseldorf, Germany

(May 2, 2019)

Abstract. The profile of a critical hole in an undercooled wetting layer is determined by the saddle-point equation of a standard interface Hamiltonian supported by convenient boundary conditions. It is shown that this saddle-point equation can be mapped onto an autonomous dynamical system in a three-dimensional phase space. The corresponding flux has a polynomial form and in general displays four fixed points, each with different stability properties. On the basis of this picture we derive the thermodynamic behaviour of critical holes in three different nucleation regimes of the phase diagram.

¹Present address: Lyman Laboratory of Physics, Harvard University, Cambridge, Massachusetts 02138

1. Introduction

The equilibrium thickness of a wetting layer on a wall is a convenient order parameter for wetting phase transitions [1]. Fig.1 shows the phase diagram for a first-order wetting transition in terms of temperature T and chemical potential μ [1]. Above the coexistence value μ_c of the two-fluid bulk system the layer thickness is infinite whereas for $h \equiv \mu - \mu_c < 0$ it is finite. In the limit $h \rightarrow 0$ from below the layer thickness continuously runs to infinity above the wetting temperature T_w , but has an infinite jump across the partial-wetting line $T < T_w$, $h = 0$. A finite jump from a thin to a thick layer occurs when the prewetting line $T_p(h)$ is crossed from the region $T < T_p(h)$ to $T > T_p(h)$. This jump runs to infinity when T_w is approached along the prewetting line and it disappears at the prewetting critical point T_{pc} .

A metastable wetting state can be generated by overheating a thin layer from $T < T_p(h)$ into a nucleation region bounded by $T_p(h)$ and an upper spinodal line $T_{us}(h)$. The transition to the stable thick-layer configuration occurs via the random formation of droplets on the thin layer and growth of the supercritical droplets [2]. Close to the prewetting line the critical droplets have a cylindrical shape with a diverging radius at $T_p(h)$. This has been pointed out by Joanny and de Gennes [3] who have chosen the name pancake droplets for this kind of critical nuclei.

It is also possible to undercool a thick wetting layer from $T > T_p(h)$ into a second

nucleation region located between $T_p(h)$ and a lower spinodal line $T_{ls}(h)$. In this case the critical nuclei are holes in the layer which near $T_p(h)$ are mirror images of the pancake droplets. Close to the partial-wetting line, however, the critical holes have a funnel-shaped profile with a diverging depth F_c but a finite inner radius R_c at $h = 0$. There exists a third regime, adjacent to the wetting transition point $T = T_w, h = 0$, at which F_c and R_c both diverge. We will refer to these regimes as the pre-dewetting, the partial-dewetting, and the complete-dewetting regime.

In order to calculate the near-coexistence behaviour of F_c, R_c , and of the excess free energy E_c of the critical hole in all regimes, we need some general information on the critical-hole profile. This is extracted from the saddle-point equation of a standard interface Hamiltonian [4] (which also determines the profile of critical droplets). As a general result this approach confirms that the size of critical nuclei diverges at the first-order lines $h = 0, T \leq T_w$ and $T = T_p(h)$, whereas it shrinks to zero at the spinodal lines.

For macroscopic critical nuclei in the region $h \approx 0, T \leq T_w$ the saddle-point equation can be mapped onto an autonomous dynamical system in a three-dimensional phase space. The flux of this system is polynomial and has a surprisingly rich fixed-point structure in the subspace of critical holes. One of these fixed points only exists, if the bulk dimension d of the system is smaller than some critical dimension d_1 . In this case there appear two different sets of physical trajectories

in the flow diagram which for $T \leq T_w$ correspond to critical holes at $h = 0$, and at $h \neq 0$, respectively. Only the latter continue to exist for $d > d_1$, and the asymptotic behaviour of their trajectories determines the T , h -dependence of F_c , R_c , and E_c . For critical holes at $h = 0$ the only nontrivial result of this kind is the T -dependence of R_c .

2. Interface model for critical holes

Our calculations are based on the Hamiltonian [4]

$$H[f] = \int d^{d-1}x \left[\frac{\gamma}{2} (\nabla f)^2 + V(f) - hf \right] \quad (2.1)$$

where $f(x)$ is the local thickness of the wetting layer on the $(d - 1)$ -dimensional planar wall of the system. The gradient term describes long-wavelength capillary excitations with a stiffness constant γ . $V(f)$ is an effective potential of the form shown in fig.2, where the repulsive core simulates the wall, and $V(f) \rightarrow 0$ for $f \rightarrow \infty$. The height of the minimum at f_{00} changes with temperature, and, in a mean-field picture, $V(f_{00}) = 0$ at $T = T_w$. Therefore, the spreading coefficient $S \equiv V(f_{00})$ can be used to measure the temperature distance from the wetting transition point [1].

In the full potential $\Phi(f) \equiv V(f) - hf$ the minimum of $V(f)$ at $f = \infty$ is, for $h < 0$, shifted to a finite value f_1 , as in fig.3. Along the prewetting line the two minima of $\Phi(f)$ have equal height, and they coincide at the prewetting critical point. The

situation of fig.3 corresponds to some point in the lower nucleation region of fig.1. At the lower spinodal line f_1 has reached the local maximum in $\Phi(f)$, changing it into a turning point.

Under the assumption of cylinder symmetry of critical holes, their radial profile $f(r)$ obeys the saddle-point equation

$$\gamma f''(r) + \frac{d-2}{r} \gamma f'(r) = dV/df(r) - h. \quad (2.2)$$

Convenient boundary conditions for such objects are $f'(r=0) = 0$ and $f(r=\infty) = f_1$ for $h < 0$ or $f'(r=\infty) = 0$ for $h = 0$, respectively. Nontrivial solutions of the latter type can in fact exist in a certain range of dimensions, as discussed below.

In order to prove the existence of critical holes inside the nucleation region at $h < 0$, we adopt an argument by Coleman [5]. He considered (2.2) as an equation of motion for a fictitious particle with position f moving in time r in a potential $-\Phi(f)$ in presence of a time-dependent friction term. At time $r = 0$ the particle has to start with zero velocity from a position f_0 such that asymptotically for $r \rightarrow \infty$ it comes to rest on top of the hill at f_1 , generating e.g. the critical-hole profile of fig.4. The existence of this marginal solution is implied by continuity from that of undershooting and overshooting solutions. Undershooting solutions obviously are produced by choosing a starting position sufficiently close to the local minimum in

$-\Phi(f)$ where the particle then eventually comes to rest. On the other hand, by choosing the starting position sufficiently close to the higher maximum in $-\Phi(f)$, the particle spends an arbitrarily long time to reach a position $f^* < f_1$, where $\Phi(f^*) = \Phi(f_1)$. This allows to neglect the friction term in the particle motion for $f > f^*$ so that by energy conservation the particle will overshoot the hill at f_1 .

Near interior points of the prewetting line $\Phi(f)$ has a double-well form which for the radial profile of a critical hole leads to a kink solution. In the limit $T \rightarrow T_p(h)$ the position R_c of the turning point of the kink runs to infinity, resembling the behaviour of a pancake droplet.

When some point on the line $h = 0$, $T \leq T_w$ is approached, f_1 and consequently the critical depth $F_c \equiv f_1 - f_0$ diverges. In this regime the critical-hole profile at macroscopic distances from the wall is determined by the asymptotic behaviour of $V(f)$ for $f \rightarrow \infty$. For long-range molecular interactions this reads

$$V(f) = Af^{1-\sigma}, \quad \text{for } \sigma > 1 \quad (2.3)$$

where A is the Hamaker constant, and $\sigma = 3$ or $\sigma = 4$ for non-retarded or retarded van der Waals forces, respectively [1]. By extrapolation the macroscopic profile $F(r)$ of a critical hole can then be defined as the solution of the differential equation

$$\gamma F''(r) + \frac{d-2}{r} \gamma F'(r) = -A(\sigma-1)F^{-\sigma} - h \quad (2.4)$$

with the new boundary conditions $F(r = R_c) = 0$ and $F(r = \infty) = F_1$ at $h < 0$ or

$F'(r = \infty) = 0$ at $h = 0$, respectively. Undershooting and overshooting solutions can still be created, now by controlling the initial velocity $F'(r = R_c)$.

Since for $r \rightarrow R_c$ the friction term and the field h can be neglected in (2.4), we find the result

$$F(r) = \left[\frac{A}{2\gamma} (\sigma + 1)^2 \right]^{\frac{1}{\sigma+1}} (r - R_c)^{\frac{2}{\sigma+1}} \quad (2.5)$$

which is asymptotically valid for all $h \leq 0$.

For $r \rightarrow \infty$ and $h \neq 0$ a linear expansion of (2.4) in $F_c - F(r)$ leads to a Bessel-type differential equation. This implies the asymptotic form

$$F(r) = F_c \left[1 - C \left(\frac{r}{R^*} \right)^{\frac{2-d}{2}} e^{-r/R^*} \right] \quad (2.6)$$

where $R^* \equiv [A\sigma(\sigma - 1)/\gamma]^{-1/2} F_c^{(\sigma+1)/2}$, and C is an integration constant. If, as an approximation to the full solution of (2.4), the expressions (2.5) and (2.6) and their derivatives are matched at some value $r = R_m$, it turns out that $R_m \sim R^*$ and C is of order 1.

For $r \rightarrow \infty$ and $h = 0$ the left-hand side in eq. (2.4) dominates for $d < d_1(\sigma)$ where

$$d_1(\sigma) \equiv \frac{3\sigma + 1}{\sigma + 1} \quad , \quad (2.7)$$

and leads to the behaviour,

$$F(r) = F^* D \left(\frac{r}{R_c} \right)^{3-d} \quad . \quad (2.8)$$

Here the amplitude $F^* \equiv [A(\sigma + 1)^2/8\gamma]^{1/\sigma+1} R_c^{2/\sigma+1}$ has been adopted from the previously derived [6] exact solution

$$\left(\frac{r}{R_c}\right)^2 - \left(\frac{F}{F^*}\right)^{\frac{\sigma+1}{2}} = 1 \quad (2.9)$$

of (2.4) at $h = 0$ in the dimension

$$d_0(\sigma) \equiv \frac{3\sigma - 1}{\sigma + 1}, \quad (2.10)$$

so that $D = 1$ in $d = d_0(\sigma)$. Due to the boundary condition $F'(r = \infty) = 0$ the asymptotic form (2.8) implies that critical holes at $h = 0$ only exist in dimensions $d > 2$. The necessity of the previously mentioned additional condition $d < d_1(\sigma)$ will become clear through the following analysis.

3. Mapping to a dynamical system

We now define the dimensionless quantities

$$\begin{aligned} X &\equiv \frac{rF'(r)}{F(r)}, \\ Y &\equiv \frac{\sigma^2 - 1}{2} \frac{A}{\gamma} \frac{r^2}{F^{\sigma+1}(r)}, \\ Z &\equiv -\frac{1}{2} \frac{h}{\gamma} \frac{r^2}{F(r)}, \end{aligned} \quad (3.1)$$

and consider their dependence on the time-like variable

$$t \equiv \ln \frac{r}{r_1} \quad (3.2)$$

where r_1 is an arbitrary reference scale. Due to (2.4) we find the set of differential equations

$$\begin{aligned}\dot{X} &= (3-d)X - X^2 - \frac{2}{\sigma+1}Y + 2Z, \\ \dot{Y} &= 2Y\left(1 - \frac{\sigma+1}{2}X\right), \\ \dot{Z} &= 2Z\left(1 - \frac{1}{2}X\right),\end{aligned}\tag{3.3}$$

which has the four fixed points

$$\begin{aligned}X_0 &= Y_0 = Z_0 = 0, \\ X_1 &= \frac{2}{\sigma+1}, \quad Y_1 = d_1(\sigma) - d, \quad Z_1 = 0, \\ X_2 &= 3-d, \quad Y_2 = Z_2 = 0, \\ X_3 &= 2, \quad Y_3 = 0, \quad Z_3 = d-1.\end{aligned}\tag{3.4}$$

For $1 < d < d_1(\sigma)$ the fixed points (3.4) are all located in the subspace $X \geq 0$, $Y \geq 0$, $Z \geq 0$, where the critical-hole trajectories occur (whereas $F'(r) \leq 0$ implies $X \leq 0$ for critical droplets). The subscripts of the fixed-point coordinates indicate the numbers of attractive principal directions of each of these points.

In the plane $Z = 0$ the fixed point P_1 in fig.5 attracts the physical trajectories coming from $X = Y = \infty$ which then either run to the droplet region $X < 0$ or to the more stable fixed point P_2 . The first possibility corresponds to undershooting solutions of the saddle-point equation whereas the second one describes solutions

obeying the boundary conditions for critical holes at $h = 0$. In fact, the fixed-point value $X_2 = 3 - d$ in connection with the definition (3.1) of X reproduces the asymptotic behaviour (2.8) up to an undetermined prefactor. In the limit $d \rightarrow d_1(\sigma)$ the fixed point P_1 merges into P_2 , and in fig.5 the right section of the basin of attraction of P_2 collapses to zero, so that critical holes at $h = 0$ no longer exist for $d > d_1(\sigma)$.

If $h < 0$, the physical trajectories approach P_1 from $X = Y = Z = \infty$ but now have three options to continue. Most of them either run into the droplet region or to the most stable fixed point P_3 , representing respectively undershooting and overshooting saddle-point solutions where the latter behave as $F(r) = -hr^2/[2(d-1)\gamma]$ for $r \rightarrow \infty$. The basins of attraction for these two sets of trajectories are separated by a surface which is the support of the critical-hole trajectories.

For $d < d_1$ the trajectories for critical holes at $h < 0$ have, contrary to our previous belief [7], no chance to come close to the fixed point P_2 (which led to the erroneous result (9) in [7]). This is a consequence of the fact that, in agreement with (2.6), these trajectories for $t \rightarrow \infty$ have to run to $X = 0, Y = Z = \infty$. According to (3.3) they must, however, penetrate the plane $X = 2/(\sigma + 1)$ above the line $Z = (2/(\sigma + 1))(Y - Y_1)$, and for $X \geq 2/(\sigma + 1)$ obey the condition $\dot{Y} \leq 0$. This is incompatible with a visit of the fixed point P_2 which consequently is supposed to have essentially no influence on the critical-hole profile for $h < 0$.

4. Critical holes at bulk coexistence

At bulk coexistence $h = 0$ there appears an infinite set of flow lines in the X, Y -plane running from $X = Y = \infty$ to the fixed point P_2 . This means that the saddle-point equation (2.4) for $h = 0$ has infinitely many solutions which obey the boundary conditions for critical holes. Only one of these solutions will, however, correspond to a true minimum in the variational principle $\delta H = 0$.

The situation can most easily be analyzed in the special dimension $d = d_0(\sigma)$.

Then, in terms of the variables

$$\eta(t) \equiv \left(\frac{r}{R_c} \right)^{-\frac{2}{\sigma+1}} F(r) \ , \ t \equiv \ln \frac{r}{R_c} \ , \quad (4.1)$$

the saddle-point equation (2.4) assumes the form [6]

$$\ddot{\eta} = -\frac{\partial}{\partial \eta} \left[\frac{A}{\gamma} R_c^2 \eta^{1-\sigma} + \frac{2}{(\sigma+1)^2} \eta^2 \right] . \quad (4.2)$$

This again can be considered as an equation of motion for a fictitious particle, now without a friction term. As a consequence the particle energy

$$\varepsilon \equiv \frac{1}{2} \dot{\eta}^2 - \frac{A}{\gamma} R_c^2 \eta^{1-\sigma} - \frac{2}{(\sigma+1)^2} \eta^2 \quad (4.3)$$

is conserved.

Eq. (4.3) can be rewritten as

$$(x-1)^2 = \frac{2}{\sigma-1} y - \lambda \frac{\sigma+1}{\sigma-1} y^{\frac{2}{\sigma+1}} + 1 \quad (4.4)$$

where

$$x \equiv \frac{X}{X_1} , \quad y \equiv \frac{Y}{Y_1} , \quad \lambda \equiv -\frac{\varepsilon}{\varepsilon_0} , \quad (4.5)$$

and $\varepsilon_0 \equiv [2/(\sigma^2 - 1)] [(\sigma - 1)(\sigma + 1)^2 AR_c^2 / (4\gamma)]^{2/(\sigma+1)}$ is the maximum value of the potential energy in (4.3). With λ taken as a parameter (4.4) analytically describes the full flow pattern of the system which is depicted in fig.6. Obviously this pattern is symmetric with respect to the line $x = 1$. For $x = y = 1$ one obtains the parameter value $\lambda = 1$ which consequently belongs to the separatrix running through the fixed point P_1 (see fig.5). This corresponds to zero kinetic energy of the fictitious particle when it passes the maximum of the potential in (4.3). Values $\lambda > 1$ accordingly belong to undershooting solutions whereas for $\lambda < 1$ one finds an infinite set of solutions obeying the critical-hole boundary conditions. The profile (2.9) leads to the value $\lambda = 0$, i.e. a simple parabola for the corresponding flow line.

For $d = d_0(\sigma)$ the energy functional $H[F(r)]$ can be written in the form $H = \Omega_{d-1} [(\sigma^2 - 1)AY_1^\sigma / (2\gamma)]^{2/(\sigma+1)} u[y]$ where

$$u = \int_0^\infty dy \frac{y^{-\frac{\sigma+3}{\sigma+1}}}{2(x-1)} \left[\frac{1}{2}x^2 + \frac{1}{\sigma-1}y \right] . \quad (4.6)$$

This implies

$$\frac{\delta u}{\delta x(y)} = \frac{1}{4}y^{-\frac{\sigma+3}{\sigma+1}} \frac{1}{(x-1)^2} \left[x^2 - 2x - \frac{2}{\sigma-1}y \right] , \quad (4.7)$$

which shows that the variational principle $\delta u = 0$ leads to (4.4) with $\lambda = 0$. The special solution (2.9) therefore, in fact, corresponds to a true minimum of H .

5. Scaling behaviour of critical holes

In order to calculate the quantities F_c , R_c , and E_c for a critical hole at arbitrary values of h , we use the definitions

$$\Phi'(F_c + f_0) = 0, \quad E_c \equiv H[f(r)] - H[F_c + f_0], \quad (5.1)$$

and extract R_c from the relation

$$\Phi(F_c + f_0) - \Phi(f_0) = (d-2)\gamma \int_0^\infty dr \frac{(f'(r))^2}{r}, \quad (5.2)$$

implied by the saddle-point equation (2.2). The second eq.(5.1) can slightly be simplified by use of the virial theorem which states that the potential-energy part in (5.1) is $(3-d)/(d-1)$ times the kinetic part. This follows from the scaling property $\partial H[f(\alpha r)]/\partial \alpha|_{\alpha=1} = 0$ which in turn is implied by the variational principle $\delta H[f_\alpha(r)] = 0$ for the special set of functions $f_\alpha(r) \equiv f(\alpha r)$. As a result of this procedure we eventually find

$$E_c = \frac{1}{d-1} \Omega_{d-1} \gamma \int_0^\infty dr r^{d-2} (f')^2 \quad (5.3)$$

where Ω_{d-1} is the volume of the $(d-1)$ -dimensional unit sphere.

Close to the line $h = 0$, $S \leq 0$, we can in (5.1)-(5.3) neglect the microscopic increment f_0 to F_c , replace $V(f)$ by its asymptotic form (2.3), and insert for $f(r)$ the macroscopic profile $F(r)$. This leads to the result

$$F_c = \frac{1}{(\sigma-1)A} |h|^{-\frac{1}{\sigma}} \quad (5.4)$$

for $h \rightarrow 0$, and, in leading order, to the equations

$$AF_c^{1-\sigma} - hF_c - S = (d-2)\gamma \int_{R_c+r_0}^{\infty} dr r^{-1} (F')^2(r), \quad (5.5)$$

$$E_c = \frac{1}{d-1} \Omega_{d-1} \gamma \int_{R_c+r_0}^{\infty} dr r^{d-2} (F')^2(r). \quad (5.6)$$

Here a cut-off length $r_0 \ll R_c$ has been introduced in order to cure the artificial singularity which due to the extrapolation (2.5) occurs at $r = R_c$ in the case $\sigma \geq 3$.

In (5.5) and (5.6) we now split off integrals running from $R_c + r_0$ to $(1 + \lambda)R_c$ wherein the choice $0 < \lambda \ll 1$ allows to use (2.5). In the remaining integrals we transform to the scaled variables r/R^* for $h < 0$ and r/R_c for $h = 0$, suggested by the asymptotic forms (2.6) and (2.8). This leads to a power in R^* and R_c , respectively, where the cofactors are assumed to be finite in the limit $h \rightarrow 0$ and $S \rightarrow 0$. The latter assumption is supported by the analysis of chapter 3 which leads to expect that no further singularities will occur in addition to those implied by (2.5)-(2.8).

On a path $S = \text{const.}$ in the partial-dewetting regime the procedure just described leads for $|h| \rightarrow 0$ to a constant value of R_c , and to

$$E_c \sim F_c^{\frac{\sigma+1}{2}(d-d_0(\sigma))} \quad (5.7)$$

with F_c given by (5.4). At $S = 0$, i.e. in the complete-dewetting regime, we find

the behaviour

$$\begin{aligned}
R_c &\sim F_c^{\frac{\sigma+1}{2}} && \text{for } \sigma < 3, \\
R_c &\sim F_c^2 \ln F_c && \text{for } \sigma = 3, \\
R_c &\sim F_c^{\sigma-1} && \text{for } \sigma > 3.
\end{aligned} \tag{5.8}$$

where again F_c has the form (5.4). Moreover, in this regime we obtain

$$\begin{aligned}
E_c &\sim R_c^{d-d_0(\sigma)} && \text{for } \sigma < 3, \\
E_c &\sim R_c^{d-2} \ln R_c && \text{for } \sigma = 3, \\
E_c &\sim R_c^{d-2} && \text{for } \sigma > 3.
\end{aligned} \tag{5.9}$$

For critical holes at $h = 0$ the only nontrivial result is the behaviour

$$\begin{aligned}
R_c &\sim |S|^{-\frac{\sigma+1}{2(\sigma-1)}} && \text{for } \sigma < 3, \\
R_c &\sim |S|^{-1} \ln |S| && \text{for } \sigma = 3, \\
R_c &\sim |S|^{-1} && \text{for } \sigma > 3
\end{aligned} \tag{5.10}$$

for $|S| \rightarrow 0$.

In the pre-dewetting regime the asymptotic behaviour of the pancake critical holes will, with growing distance from T_w , increasingly depend on the microscopic details of the potential $\Phi(f)$. We therefore have to go back to the relations (5.2) and (5.3), in which we then use the fact that $f'(r)$ is sharply peaked at the value $r = R_c$. This leads for any path $S = \text{const.}$ to a constant value of F_c at the prewetting line

$h = h_p(T)$, and to the relations

$$R_c \sim (h_p(T) - h)^{-1}, \quad (5.11)$$

$$E_c \sim (h_p(T) - h)^{2-d} \quad (5.12)$$

which are identical to those for pancake droplets [3]. When the wetting transition point is approached along the prewetting line, F_c diverges as in (5.4).

The crossover lines, separating the pre-dewetting and the partial-dewetting regime from the intervening complete-dewetting regime (see fig.1), are of the form $|h| \sim |S|^{\frac{\sigma}{\sigma-1}}$. This is implied by eq. (5.5) through which the spreading coefficient S enters the calculation in the form $S + \text{const}|h|^{\frac{\sigma-1}{\sigma}}$.

Some of the results (5.4),(5.7)-(5.12) should be accessible to experiments, although (5.10) strictly applies only to $d < d_1(\sigma)$. For general d the behaviour (5.10) might, however, be observable on a path $h = \text{const} \lesssim 0$ in the partial-dewetting regime. The relevance of the behaviour (5.7) has been pointed out previously [8] in connection with the observed anomalously long lifetimes of undercooled wetting layers [9]. Direct observations of the nucleation of holes in wetting layers have also been reported in the recent literature [10].

Acknowledgement. We are grateful to R. Burghaus for many helpful discussions. This work has been supported by the DFG under SFB 237 “Unordnung und Große Fluktuationen”.

References

- [1] P.G. de Gennes, *Rev. Mod. Phys.* **57**, 825 (1985); S. Dietrich, in *Phase Transitions and Critical Phenomena*, eds. C. Domb and J.L. Lebowitz, vol. 12 (Academic Press, London, 1988).
- [2] R. Bausch, R. Blossey, *Europhys. Lett.* **14**, 125 (1991); *Phys. Rev.* **E48**, 1131 (1993);
- [3] J.F. Joanny, P.G. de Gennes, *C.R.Acad.Sc.Paris*, **303II**, 337 (1986);
- [4] E. Brézin, B.I. Halperin and S. Leibler, *J. Phys. (Paris)* **44**, 775 (1983); R. Lipowsky, D.M. Kroll and R.K.P. Zia, *Phys. Rev.* **B27**, 4499 (1983);
- [5] S. Coleman, in *Aspects of Symmetry*, Cambridge University Press, Cambridge (1985);
- [6] M. Burschka, R. Blossey and R. Bausch, *J. Phys.* **A26**, L1125 (1993); R. Bausch, R. Blossey, M.A. Burschka, *J. Phys.* **A27**, A1405 (1994);
- [7] R. Bausch, R. Blossey, G. Foltin, *Physica* **A224**, 93 (1996);
- [8] R. Bausch, R. Blossey, *Phys. Rev.* **E50**, R1759 (1994);
- [9] J.E. Rutledge, P. Taborek, *Phys. Rev. Lett.* **69**, 937 (1992); D. Bonn, H. Kellay and J. Meunier, *Phys. Rev. Lett.* **73**, 3560 (1994);
- [10] see, e.g., the review by R. Blossey, *Int. J. Mod. Phys.* **B9**, 3489 (1995), and more recently P. Lambooy, K.C. Phelan, O. Haug, and G. Krausch, *Phys. Rev. Lett.* **76**, 1110 (1996), J. Bishof, D. Scherer, S. Herminghaus, and P. Leiderer, *Phys. Rev. Lett.* **77**, 1536 (1996).

Figure Captions

Figure 1: T, μ -phase diagram for a first-order wetting transition. All symbols are explained in the introduction. The shaded area is the complete-dewetting regime, separated by crossover lines from the partial- and pre-dewetting regimes.

Figure 2: The effective interface potential $V(f)$, where $S \equiv V(f_{00})$.

Figure 3: The full potential $\Phi(f) \equiv V(f) - hf$. Here, f_1 is the equilibrium thickness of the undercooled layer, and $f_1 - f_0$ is the depth of the critical hole.

Figure 4: The profile of the critical hole corresponding to the potential in fig.4.

Figure 5: The flow diagram of the dynamical system (3.3) with all fixed points and their principal directions. The shaded region is the sector in the plane $X = 2/(\sigma+1)$ penetrated by the physical trajectories for $h < 0$.

Figure 6: The flow pattern corresponding to eq. (4.4) for the limiting case $\sigma = 3$ (note that $F'(r = \infty) = 0$ for $\sigma = 3$).

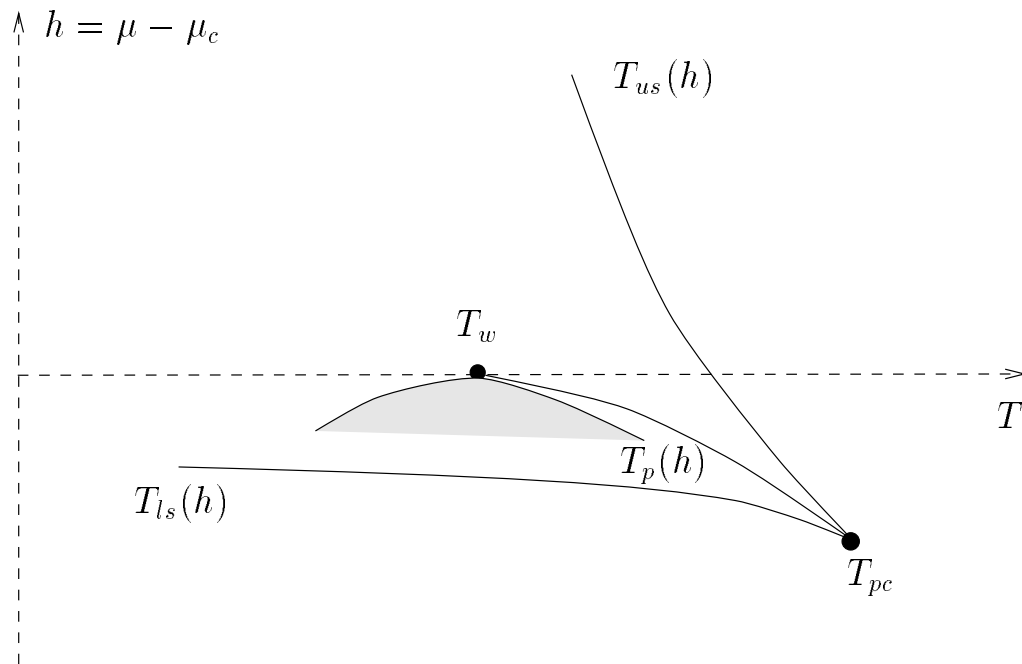


Figure 1

Foltin et al.

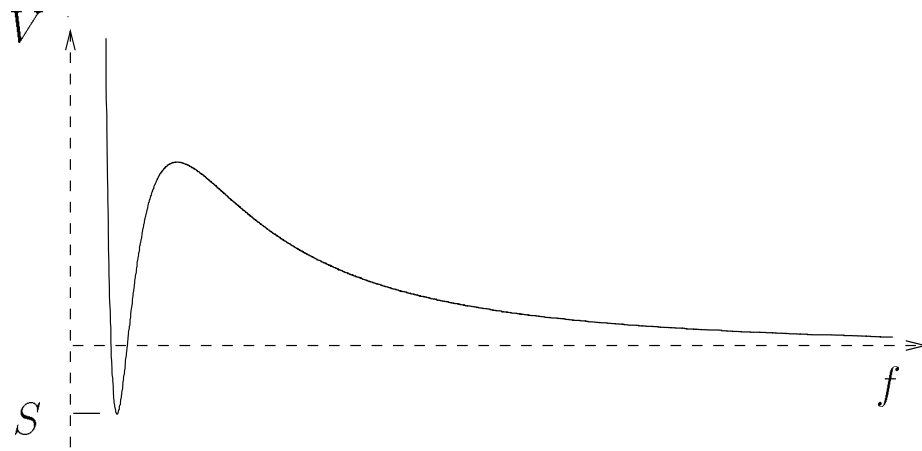


Figure 2

Foltin et al.

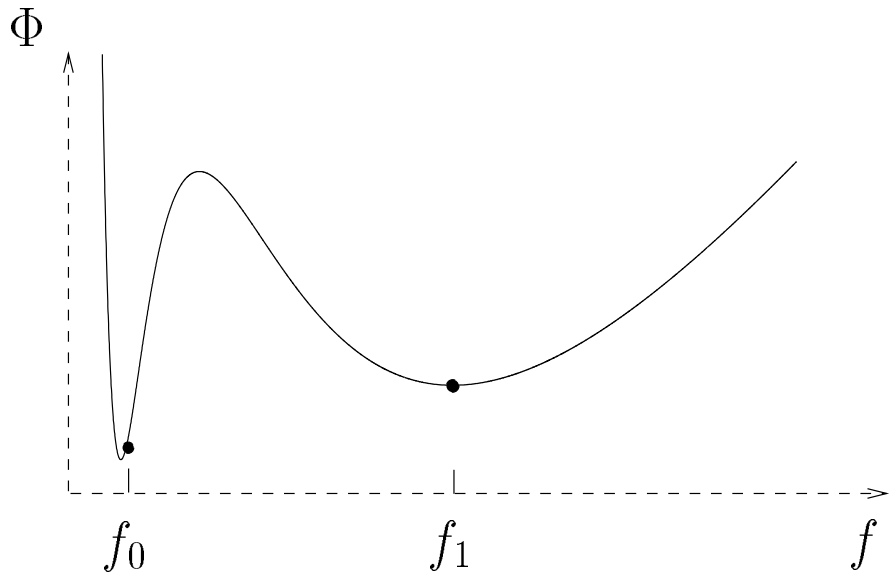


Figure 3

Foltin et al.

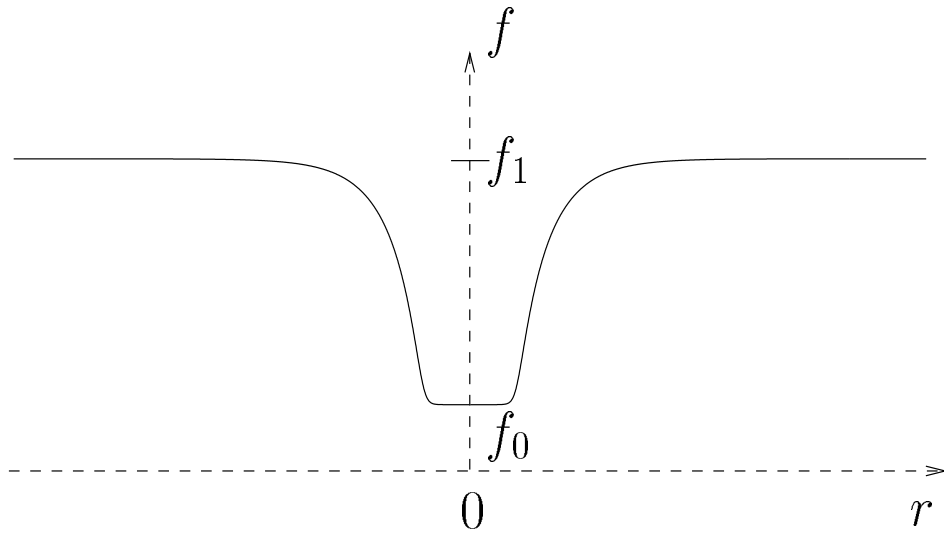


Figure 4

Foltin et al.

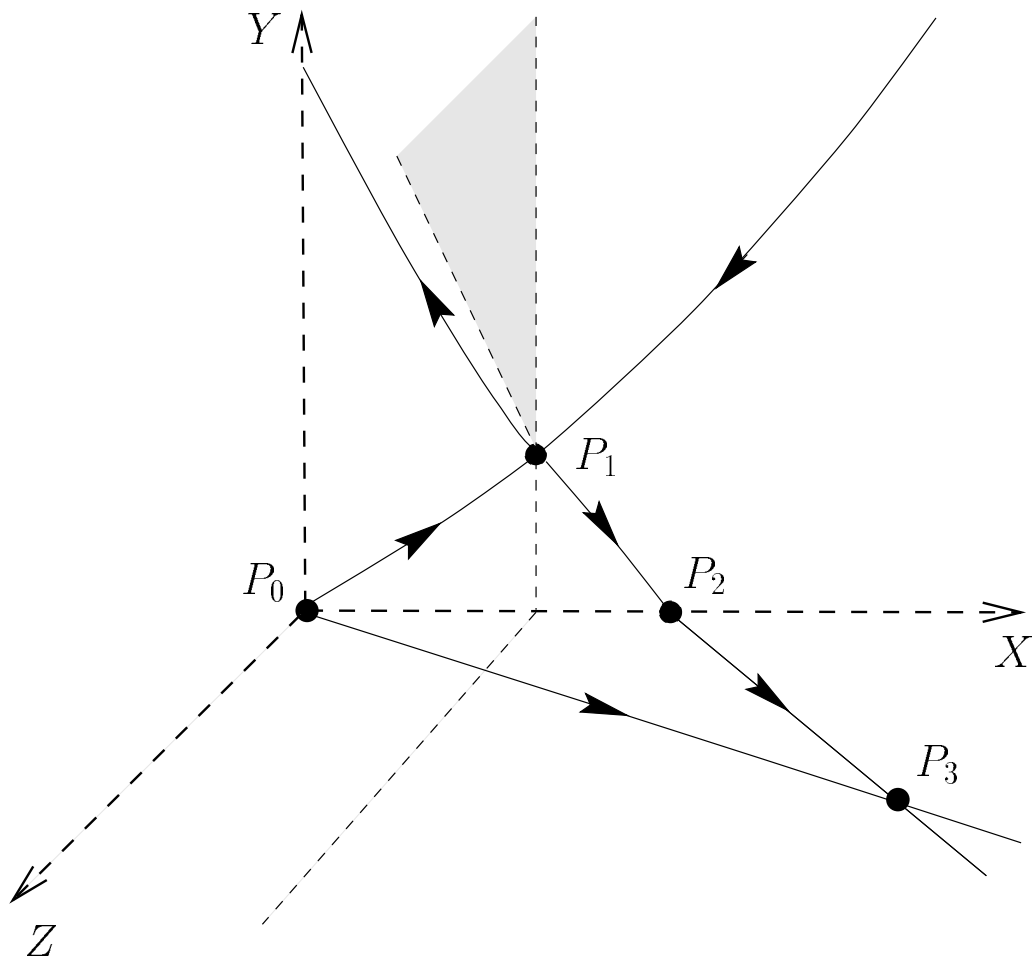


Figure 5

Foltin et al.

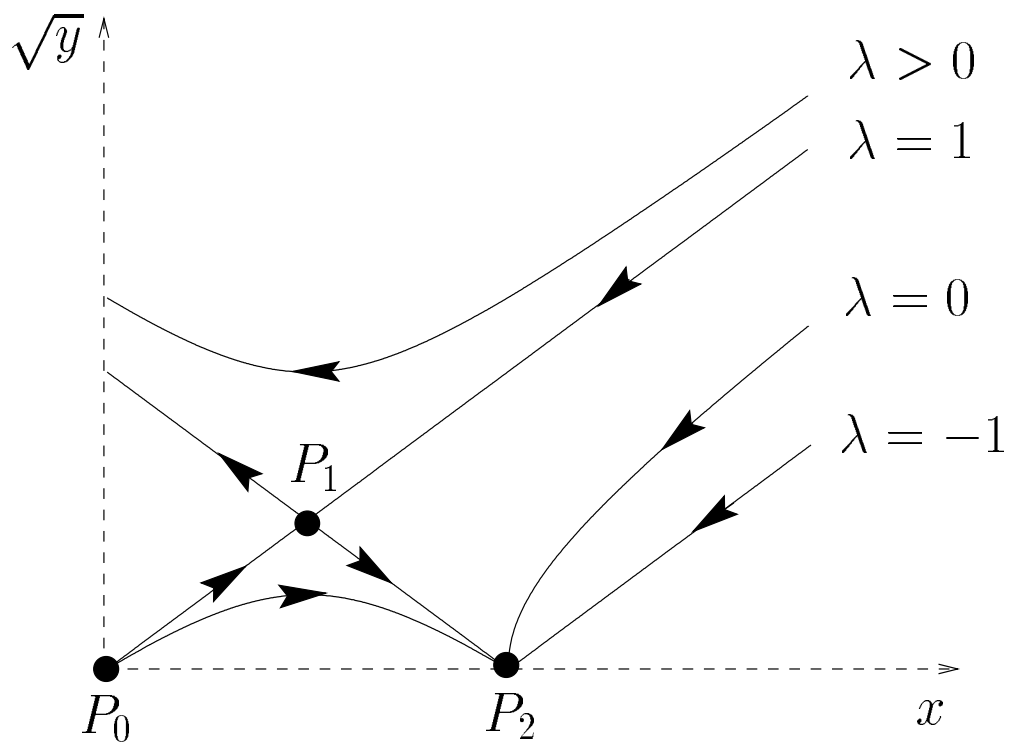


Figure 6

Foltin et al.